Building and Environment 187 (2021) 107360

Contents lists available at ScienceDirect

Building and Environment

journal homepage: http://www.elsevier.com/locate/buildenv

Spatial seated occupancy detection in offices with a chair-based temperature sensor array

Danielle N. Wagner [a,b], Aayush Mathur [b,c], Brandon E. Boor [a,b,*]

[a] Lyles School of Civil Engineering, Purdue University, West Lafayette, IN, 47907, USA
[b] Ray W. Herrick Laboratories, Center for High Performance Buildings, Purdue University, West Lafayette, IN, 47907, USA
[c] School of Mechanical Engineering, Purdue University, West Lafayette, IN, 47907, USA

ARTICLE INFO

Keywords:
Occupancy sensing
Indoor environmental quality
Occupancy profiles
HVAC control
Occupant behavior
Sensors

ABSTRACT

Sensors used to monitor indoor environmental conditions and utility consumption can result in well-defined working and living spaces. Real-time spatiotemporal occupancy detection techniques used to track humans indoors paired with these data can be used to better understand the role of occupants on indoor air quality and building energy consumption. This study introduces a novel occupancy sensing technique whereby a chair-based temperature sensor array is used to detect the presence of occupants seated in a living laboratory open-plan office. Seat surface temperatures were tracked for twenty individuals over seven months using K-type thermocouples with battery-powered dataloggers secured to office chairs in known locations. The temperature differential between the occupant and seat surface enables for rapid conduction and thus detection of one's seated presence. Seat surface temperature time-series were converted to binary seated occupancy for each chair and totaled to achieve a spatial map of room seated occupancy with a time resolution of 15 s. Trends in spatiotemporal seated occupancy profiles in the office were evaluated for seven months using the novel technique. This highly localized form of occupancy detection offers several advantages compared to delocalized sensing techniques, including visualization of spatial occupancy patterns over time; determination of individual seated occupancy histories visualized in the form of "occupancy barcodes; " quantification of total seated hours per occupant in different spatial zones across varying time-scales; and characterization of diurnal and weekly trends in seated occupancy probabilities categorized by an occupant's relative level of presence.

1. Introduction

1.1. Motivation for occupancy detection in buildings

Building design and operation intending to maximize occupant performance must more rigorously explore the complex relationships that exist when occupants interact with their built surroundings. An important element underlying this aim is the evaluation of human occupancy patterns in buildings. Occupancy detection enables for assessment of human behavior and activity patterns. Such assessments can be used to better understand how people influence indoor air quality and building energy consumption. Integration of occupancy sensors with building automation systems offers a basis to provide personalized heating and cooling to improve occupant comfort and productivity [1–3]. Occupancy data can enable building systems to more accurately address ventilation and energy needs throughout the day. Establishing scalable systems for detecting human occupancy provides a foundation for optimizing indoor environmental quality and energy usage expenditures through smart control of heating, ventilation, air conditioning, and lighting (HVAC&L) systems.

Humans continually emanate bioeffluents and dissipate heat and moisture, thereby having a measurable impact on indoor environments. Monitoring occupancy patterns in buildings can help to better understand how people alter the microbial and chemical composition of indoor air. Concentrations of human-associated species are often correlated with occupancy levels and tend to scale with the number of occupants in an indoor space for a fixed ventilation rate [4–7]. People continually shed bacteria and fungi from their skin and clothing and stir-up settled dust from indoor surfaces via resuspension as they move around [6,8–11]. Occupants are the primary source of carbon dioxide (CO_2) indoors. CO_2 is a major constituent of exhaled breath and the most common surrogate for occupancy. In addition to CO_2, the human body

* Corresponding author. Lyles School of Civil Engineering, Purdue University, West Lafayette, IN, 47907, USA.
E-mail address: bboor@purdue.edu (B.E. Boor).

https://doi.org/10.1016/j.buildenv.2020.107360
Received 22 July 2020; Received in revised form 15 September 2020; Accepted 4 October 2020
Available online 6 October 2020

releases hundreds of volatile organic compounds (VOCs) via exhaled breath, skin secretions, squalene ozonolysis, and personal care products [12–20]. Measured species concentrations can be integrated with occupancy data to determine emission or generation rates per person in order to quantify the impact of humans on indoor air quality [17,21,22]. Occupancy monitoring offers a basis for improved population exposure assessment for indoor air species that can adversely affect respiratory and cardiovascular health, impair cognitive function and decision making, and cause fatigue, headache, and sleepiness [23–26].

Given the prominent role humans play in altering the composition of indoor air, real-time occupancy detection is an important element in mechanical ventilation control strategies for buildings. Ventilation standards, such as ANSI/ASHRAE Standard 62.1–2019, outline the volumetric flow rate of filtered outdoor air per person that must be delivered to an occupied space to maintain acceptable concentrations of indoor air species [27]. In indoor spaces where occupancy patterns are temporally variant, such as open-plan offices, meeting rooms, common areas, and classrooms, the outdoor air ventilation rate should be dynamically modulated to prevent the accumulation of human-associated CO_2, VOCs, and particles. Demand controlled ventilation (DCV) is one technique that addresses the need for occupant-driven outdoor air ventilation requirements in small- and large-scale office buildings by introducing more filtered outdoor air into a room when more people are present. In addition to affecting indoor air quality, implementation of DCV offers benefits in regard to energy savings [28], which have been found to range from 8 to 80%, depending on the season, location, and worker schedules [29].

Occupancy-based control of HVAC&L systems in buildings can enable for optimization of indoor environmental quality and energy usage by considering worker needs and schedules rather than by applying a one-size-fits-all timetable. Real-time occupancy sensing is therefore an important element in achieving human-centered building design and operation. Given the diversity of indoor environments and complexity of human behavior patterns, predicted occupancy profiles do not always align with actual occupancies. This can result in the heating, cooling, and artificial illumination of vacant rooms [30,31], or conversely, insufficient conditioning or ventilation of over-occupied spaces. Live occupancy trends at the room- and building-scale offers the potential for energy savings through more intelligent control over HVAC&L operations [2,31–35]. Demand-driven control in smart buildings can be tailored to a specific indoor environment either through real-time automation or short-term learning to predict occupancy patterns and adjust setpoint schedules accordingly. In addition to HVAC&L control, robust occupancy data is an important input for indoor air quality and building energy models that consider the impact of people on shaping their proximate indoor environments [36].

Smart control of HVAC&L systems that more deeply considers occupancy patterns and individual preferences necessitates development and integration of occupancy sensing techniques that consider specific environments and predict their end-use format. Wireless devices interacting with each other and a central hub via the Internet of Things (IoT) brings an interconnectedness between building control, sensors, and room conditions that enables for optimal control based on immediate occupant feedback [33,37,38]. Localized occupancy sensing platforms that monitor an individual's occupancy time-series can be integrated with IoT-based building automation systems to achieve occupant-centric indoor spaces.

Occupancy detection has applications beyond indoor environmental quality and building energy use. Seated occupancy sensing can inform time spent in sedentary activities indoors, such as working in front of a computer. Sedentary activities have been estimated to require 30–50% less energy than standing-related or more intense actions; and more time spent seated can offset the benefits of routine exercise. In office environments, studies have shown that workers sit longer than recommended – for approximately 66–77% of their total work time [39–41] or 4–9 h per day. Extensive sitting is likely to continue outside of the workplace [42]. The act of continuous sitting itself has detrimental effects on metabolism and mortality [43]. People who spend more time sitting are also those that spend less time active and tend to be older [44]. Explorations of seated times for workplace interventions intended to encourage physical activity during the workday often use thigh-attached or inclination-based accelerometers [43–47] and self-reporting techniques [42,48,49]. These studies advocate management methods that encourage workers to perform certain tasks or furniture modifications, such as using stand-up desks, to facilitate more frequent standing and movements. Localized occupancy estimates combined with information about individual needs and indoor environmental quality can inform building design and operation to mediate unwanted, unhealthy outcomes of occupant-office interactions.

1.2. Occupancy sensing techniques

Technological advancements resulting in smaller and more affordable sensors that measure concentrations of indoor air species, monitor indoor environmental conditions, track movement, register images, detect electronic devices, and assess seat parameters have allowed a plethora of investigation into people and their effects on building management. Methods used to understand the relationship between occupants and the indoor environment ideally determine the count, location, behavior, and timing of people in a given space, often using a combination of sensors. Papers by Horr et al. (2016), Labeodan et al. (2016), and Yang et al. (2016) have recently surveyed occupancy sensing techniques for buildings [50–52]. Most sensing techniques can accurately detect presence or room count to a high degree with the right understanding of a room setup and using well-tuned algorithms to match sensor output to occupant counts. Utilizing training data, machine learning, or a combination of sensors often improves the accuracy of the technique employed.

One of the most common forms of occupancy detection in buildings is CO_2 sensing. CO_2 sensors are frequently integrated with DCV [37,50,53–61]. Complete mixing of CO_2 in an occupied space is often assumed and steady-state CO_2 concentrations are commonly estimated using constant CO_2 generation rates per person and constant outdoor air concentrations [62]. While CO_2-based occupancy sensing has been shown to estimate occupancy with accuracies ranging from 55 to 95% [54], notable assumption flaws in using CO_2-driven ventilation suggest a need for improved occupancy sensing techniques. These uncertainties include but are not limited to occupancy detection time delay [51]; sensor error in determination of accurate CO_2 concentrations; occupancy mischaracterization due to sensor placement within a room [63]; variable outdoor air conditions; overgeneralizing outdated CO_2 generation rates for different levels of physical activity [62]; health-based CO_2 concentration thresholds [64]; and poor prediction of concentrations of other human-associated species, such as VOCs and particles [39]. The U. S. Department of Energy notes that CO_2-based DCV introduces a period of lag and an occupancy buffer where extra outdoor air is delivered to unoccupied spaces [65]. CO_2 is commonly measured at one location per room, thereby preventing determination of spatial occupancy patterns within the room. Modeling techniques to improve the accuracy of CO_2-based occupancy sensing have been proposed [60]. In addition to CO_2, concentrations of human-associated VOCs and particles can be used to evaluate temporal occupancy patterns [9,10,17,21,58,66–68].

Occupancy sensing techniques relying on physical movement include traditional usage of passive infrared (PIR) for light automation and multiple sensors placed in doorways that count instances of presence and determine directionality to estimate total occupancy [54,58,69–72]. Cameras have been used in a similar manner, however, they may illicit questions of privacy [54,69,73,74]. Acoustics have been used to infer occupancy, both by exploring the novel use of filtered speech-based audio and by looking at general room noise [37,58,75,76]. Additional indoor environmental parameters that have been tested to detect occupant presence include indoor air temperature and relative

humidity and light [54,58,77].

Device-centered occupancy sensing assumes that people are continually "plugged in" to their electronics. Device detection methods are based on the tracking of WiFi and Bluetooth signals via Media Access Control (MAC) and Internet Protocol (IP) addresses. A spatial map of electronic devices in an indoor space can be generated based on each device's distance from a grid of receivers correlated with signal strength [35,73,77–79]. Once enabled, delocalized sensors can continuously yield relatively accurate zone-based occupancy patterns over time, however, they may not always identify exact placement in a building due to variations in electronics and room environments [60,62,73,77]. A similar exploration of literal human detection was proven to detect radio wave emissions from people [80,81].

Seat- or chair-based occupancy determination enables for multi-point tracking of occupants within an indoor space. Due to the sensitivity of movement when one sits, chairs have been successfully outfitted with sensors based on acceleration to monitor seated occupancy and to identify seated activities [46,47]. Capacitance and micro-switch-based pressure have also been used to note when an individual is present with detection accuracy ranging from 80 to 100% depending on the room and sensor setup [34,53,78,82–84]. Using arrays of these sensors can help determine where a seated person is within a room, as well as an individual's posture or specific activities [85–89]. When individual locations are known at given times, the total seated occupancy can then be calculated. While accurately detecting occupant presence, pressure sensors may overestimate seated occupancy when inanimate, non-living objects are placed in seats [90]. People may place blankets, backpacks, and other items in car seats and classroom and office chairs; therefore, using a sensor that is more adept to specifically sensing humans avoids false-positives due to item storage. Occupant self-reporting has been used to supplement chair-based sensor measurements and introduces biases of occupancy timing by underreporting absences [91].

1.3. A chair-based temperature sensor array for spatiotemporal occupancy detection in offices

This study investigates the use of a chair-based temperature sensor array for spatiotemporal occupancy detection in open-plan offices. The use of chair-based temperature sensors (e.g. thermocouples) to monitor seated occupancy in buildings has not been previously explored to the best of the authors' knowledge. The temperature differential between a seated person and seat cushion enables for rapid heat transfer via conduction and thus detection of one's seated presence. Thermocouples embedded in, or attached to, chair cushions are a viable option to determine seated occupancy in indoor environments where people are seated the majority of the time, such as offices, classrooms, theaters, and public transportation. Russell et al. (2017) used arrays of thermocouples embedded in seat cushions to detect seated postures, demonstrating a thermocouple's sensitivity to someone sitting, standing, and repositioning in one's seat [86].

The primary objective of this study is to introduce a novel technique for highly localized occupancy sensing in offices – a chair-based temperature sensor array – and demonstrate the utility of the technique in evaluating spatiotemporal seated occupancy profiles through a 7-month measurement campaign in a living laboratory open-plan office. K-type thermocouples were appended to the seat cushions of twenty office chairs in known locations (Fig. 1). The paper first presents the methodology for converting seat surface temperature time-series to binary seated occupancy and then aggregating across the entire office to determine the total seated occupancy in the room. The paper then discusses how the technique enables for detailed assessment of both spatial and temporal seated occupancy patterns in the office over varying timescales.

2. Material and methods

2.1. Chair-based temperature sensing in a living laboratory open-plan office

Occupancy measurements with the chair-based temperature sensor array were conducted in the Herrick Living Laboratories of the Center for High Performance Buildings at Purdue University in West Lafayette, Indiana from February 10 to August 31, 2019. The Living Labs are four nearly identical, side-by-side large open-plan office spaces for graduate students with reconfigurable and precisely controlled envelope, lighting, and thermal systems. The chair-based temperature sensor array was deployed in the Living Lab office that regularly contained the highest number of occupants. The office contained 20 assigned desks and chairs arranged as a grid of 4 rows with 5 desks each (Fig. 1) (L: 10.50 m, W: 9.9 m, H: 4.60 m). Each desk and chair were given a numeric ID of 1 through 20 to ensure desk-chair location continuity and to de-identify data. It is assumed the same person was assigned a given desk-chair pair for the entirety of the measurement campaign. Observations indicated the occupants remained seated, aside from short periods of

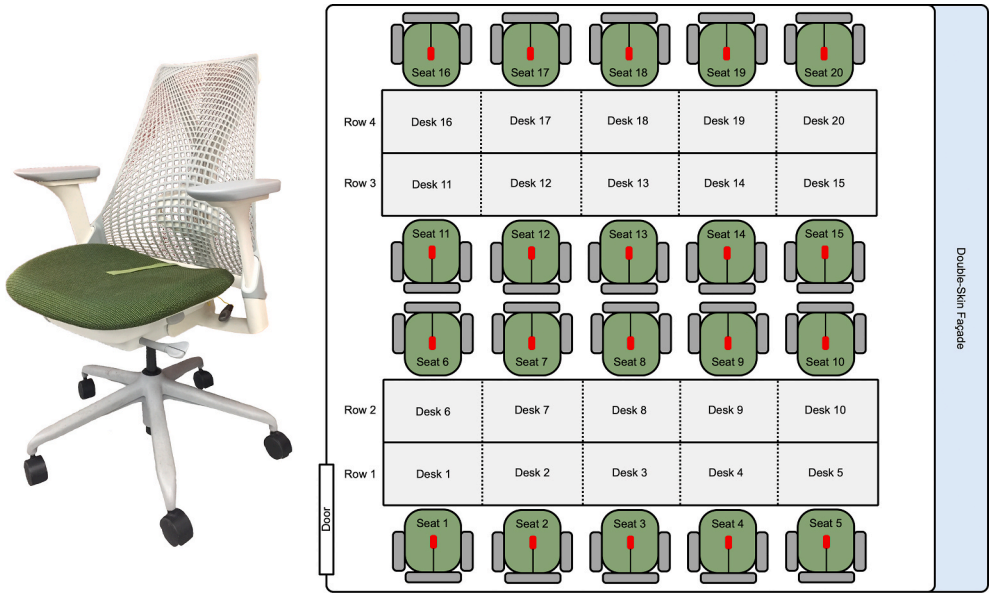

Fig. 1. (left) photo of a Living Lab office chair configured with a fabric-covered K-type thermocouple connected to a battery-powered datalogger and (right) illustration of the chair-based temperature sensor array in the Living Lab open-plan office. Each seat surface temperature sensor node is shown in red. The associated numeric ID (1–20) for the given desk-chair pair location is listed, along with the desk row number (1–4). (For interpretation of the references to color in this figure legend, the reader is referred to the Web version of this article.)

standing entry and exit and group discussions. As such, all results presented herein are referred to as "seated occupancy" for correctness.

The chair-based temperature sensor array was created by configuring each chair with a K-type epoxy coated tip thermocouple (TC-PVC-K-24-180, Omega Engineering Inc.) connected to a battery-powered datalogger (EasyLog EL-USB-TC, Lascar Electronics Inc.). The thermocouple was positioned at the middle of the upward-facing seat cushion and attached to the cushion with double-sided fabric tape (Fig. 1). The cable was directed to the rear of the chair and covered with fabric tape of the same color as the cushion. The datalogger was attached to the bottom of the chair cushion with Velcro to enable for repetitive removal for data acquisition twice per week. Seat surface temperatures (in °C) for all 20 chairs were recorded with 15-s time resolution for the duration of the 7-month occupancy measurement campaign, aside from a 1.5-week period in mid-July 2019 (parts of weeks 29 and 30).

2.2. Determination of seated occupancy via seat surface temperature profiles

Measured seat surface temperature time-series, $T_m(t)$, were used to determine seated occupancy time-series with 15-s time resolution for each chair within the spatial grid of the Living Lab office (Fig. 1). The measured seat surface temperatures were compared to the median seat surface temperature for each chair, $\overline{T}_m$, calculated for a given data acquisition period (3–4 days). Here, $\overline{T}_m$ is treated as the background seat surface temperature given that the chairs were occupied for approximately one-third or less of the total measurement period. The range of $\overline{T}_m$ was generally between 22 and 23 °C throughout the measurement campaign.

$T_m(t)$ was referenced to $\overline{T}_m$ to enable for additional reduction of the seat surface temperature time-series. This reduction step was done to facilitate occupancy determination whereby sudden increases in the seat surface temperature above $\overline{T}_m$, often approaching and exceeding 30 °C, were attributed to occupant seated presence due to heat transfer via conduction from the person to the chair surface. Reduced seat surface temperature time-series, $T_r(t)$, were computed as follows:

$$T_r(t) = \begin{cases} \overline{T}_m, \text{ if } T_m(t) \leq \left(\overline{T}_m + 3^\circ C\right) \\ T_m(t), \text{ if } T_m(t) > \left(\overline{T}_m + 3^\circ C\right) \end{cases} \quad (1)$$

$T_r(t)$ was used to create a binary seated occupancy time-series, $O_s(t)$, for each chair, with 0 indicating absence of the occupant and 1 indicating seated presence of the occupant. During periods of stable seated occupancy, $T_r(t)$ is often between 34 and 36 °C. Binary seated occupancy for each chair was calculated with 15-s time resolution as follows:

$$O_s(t) = \begin{cases} 0, \text{ if } T_r(t) = \overline{T}_m \\ 1, \text{ if } T_r(t) > \overline{T}_m \\ 0, \text{ if } O_s(t) = 1 \text{ and } \overline{T}_m < T_r(t + \Delta t) < 30^\circ C \end{cases} \quad (2)$$

The third criteria accounts for sudden decreases in the seat surface temperature when a person stands up following a period of seated occupancy (e.g. Fig. 2a at 17:00). During such conditions, $T_r(t)$ can remain above $\overline{T}_m$ u ntil the seat surface temperature decays to background. Thus, $O_s(t)$ is corrected from 1 to 0 when $T_r(t+\Delta t)$ falls below 30 °C, while remaining above $\overline{T}_m$, where Δt is equal to one sampling interval of 15 s. Binary seated occupancy time-series for each chair within the spatial grid of the Living Lab office were computed for the duration of the 7-month occupancy measurement campaign. It is assumed that seated occupants remained in direct contact with the thermocouple during periods of seated occupancy and that people are the only heat

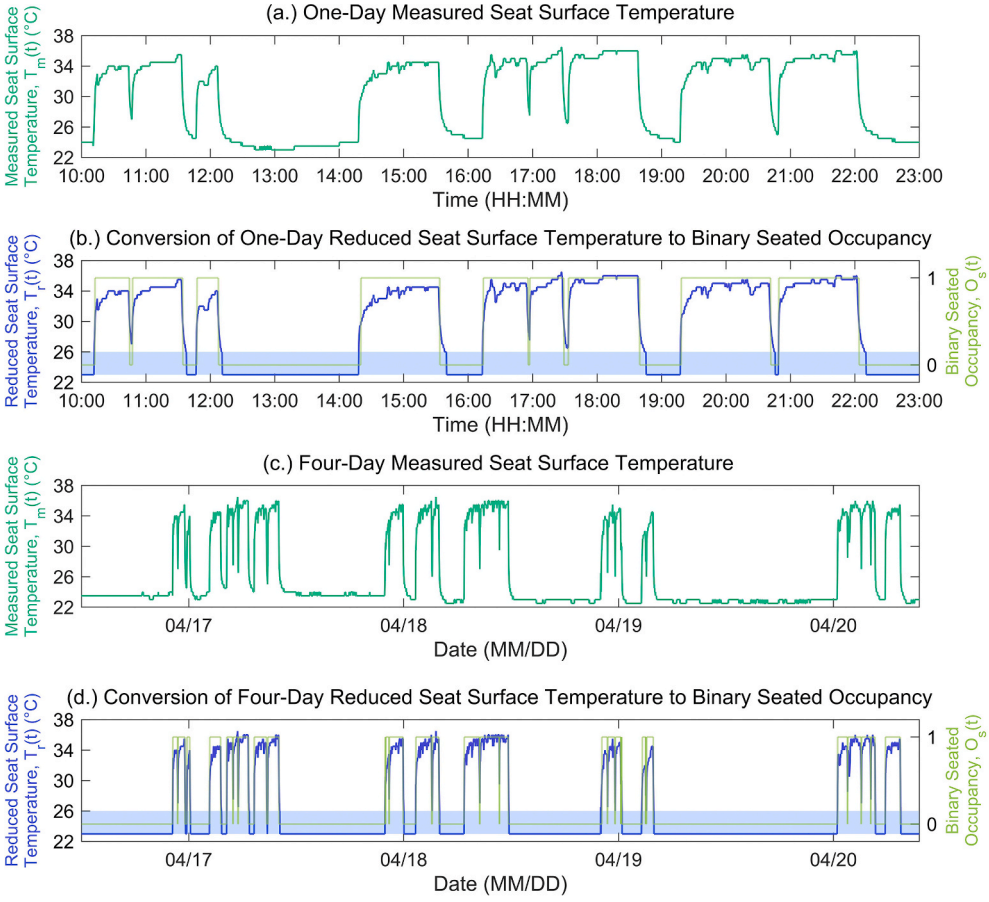

Fig. 2. Example of binary seated occupancy determination via chair-based temperature sensing for one chair in the open-plan office: (a.) one-day measured seat surface temperature time-series, $T_m(t)$, (b.) one-day reduced seat surface temperature time-series, $T_r(t)$ (left y-axis) and one-day binary seated occupancy time-series, $O_s(t)$ (right y-axis), (c.) four-day measured seat surface temperature time-series, $T_m(t)$, and (d.) four-day reduced seat surface temperature time-series, $T_r(t)$ (left y-axis) and four-day binary seated occupancy time-series, $O_s(t)$ (right y-axis). $O_s(t) = 0$ for seated absence and $O_s(t) = 1$ for seated presence. The blue bands in (b.) and (d.) are bounded by $\overline{T}_m$ (lower) and $\overline{T}_m + 3^\circ C$ (upper), where $\overline{T}_m = 23$ °C. (For interpretation of the references to color in this figure legend, the reader is referred to the Web version of this article.)

source in direct contact with the chair cushion. Periodic manual reporting of binary seated occupancy was conducted to guide the criteria established in Equations (1) and (2) and to verify the accuracy of the occupancy determinations derived from the seat surface temperature data.

The total seated occupancy in the Living Lab office, $O_{s,total}(t)$, was taken as the sum of the binary seated occupancies for each of the 20 chairs:

$$O_{s,total}(t) = \sum_{\text{Seat } 1}^{\text{Seat } 20} O_s(t) \tag{3}$$

3. Results

3.1. Spatial and temporal seated occupancy data analysis and visualization

The chair-based temperature sensor array was deployed in the Living Lab office for 7 months to evaluate the utility of the new occupancy sensing technique in tracking seated occupancy patterns at varying spatial scales (chair, row, room) and temporal scales (hour, day, week, month). Regarding spatial occupancy monitoring in an open-plan office environment, this highly localized form of occupancy detection presented several unique attributes compared to delocalized sensing techniques, such as a single CO_2 or door PIR sensor per office. First, individual seated occupancy histories were calculated for each of the 20 desk-chair pairs for the duration of the measurement campaign. The binary $O_s(t)$ time-series for each chair (0–1) were visualized in the form of "occupancy barcodes" to provide a basis to identify long-term, month-to-month trends in seated occupancy (Fig. 3). Second, the $O_s(t)$ time-series for each chair were integrated with respect to time, $\int O_s(t)\,dt$, to quantify the total seated hours per occupant in different spatial zones (chair, row) across varying time-scales. As the desk-chair pairs were assigned to 20 occupants and arranged in a grid of 4 rows with 5 desks each (Fig. 1), this enables for creation of spatial maps of the total time seated in each chair for each month and for the entirety of the measurement campaign (Fig. 4).

Third, diurnal and weekly trends in the total seated occupancy, $O_{s,total}(t)$, were characterized at the spatial-scale of the entire room. Diurnal trends in $O_{s,total}(t)$ were aggregated to calculate mean and median characteristic seated occupancy profiles for the office for weekdays (Monday to Friday) and weekends (Saturday and Sunday) (Fig. 6). Fourth, as this technique tracks chair-specific seated occupancy patterns in a shared, multi-user indoor workspace, individual occupancy trends ($O_s(t)$) can be compared to the combined whole ($O_{s,total}(t)$). Each of the 20 chairs were ranked based the occupant's relative level of seated presence over the measurement campaign as follows: (1.) high: seated occupancy greater than the 80th percentile, (2.) medium: seated occupancy between 20th and 80th percentiles, and (3.) low: seated occupancy less than the 20th percentile (Fig. 9). Diurnal and weekly seated occupancy profiles were calculated for each of the three categories to demonstrate how this sensing technique can be used to cluster occupants based on relative time spent in the office.

3.2. Evaluation of binary seated occupancy determination via chair-based temperature sensing

Binary seated occupancy time-series, $O_s(t)$, were calculated from measured seat surface temperature time-series, $T_m(t)$, for each of the 20 chairs in the Living Lab office for the duration of the 7-month measurement period. Fig. 2 shows measured ($T_m(t)$) and reduced ($T_r(t)$) seat surface temperature profiles and the corresponding $O_s(t)$ for one chair over two time-scales (1 day and 4 days). Fig. 2 serves as an illustrative example of the temporality in $T_m(t)$ and $T_r(t)$ and how $T_r(t)$ was converted to $O_s(t)$. The blue band in Fig. 2b and d is bounded by $\overline{T}_m$ and $\overline{T}_m + 3°C$, both of which are used to define the reduction from $T_m(t)$ to $T_r(t)$. For $T_m(t) > \left(\overline{T}_m + 3°C\right)$, both the measured and reduced temperatures are identical, whereas for $T_m(t) \leq \left(\overline{T}_m + 3°C\right)$, the reduced temperature transitions to $\overline{T}_m$.

It can be seen that the reduction from $T_m(t)$ to $T_r(t)$ coverts background seat surface temperatures to a constant $\overline{T}_m$, thereby aiding in identification of seated periods when $T_r(t) > \overline{T}_m$. When an occupant sits on the seat cushion of a chair, $T_r(t)$ tends to rise logarithmically from $\overline{T}_m$ to over 30 °C. During continued seated occupancy in the chair, temporal

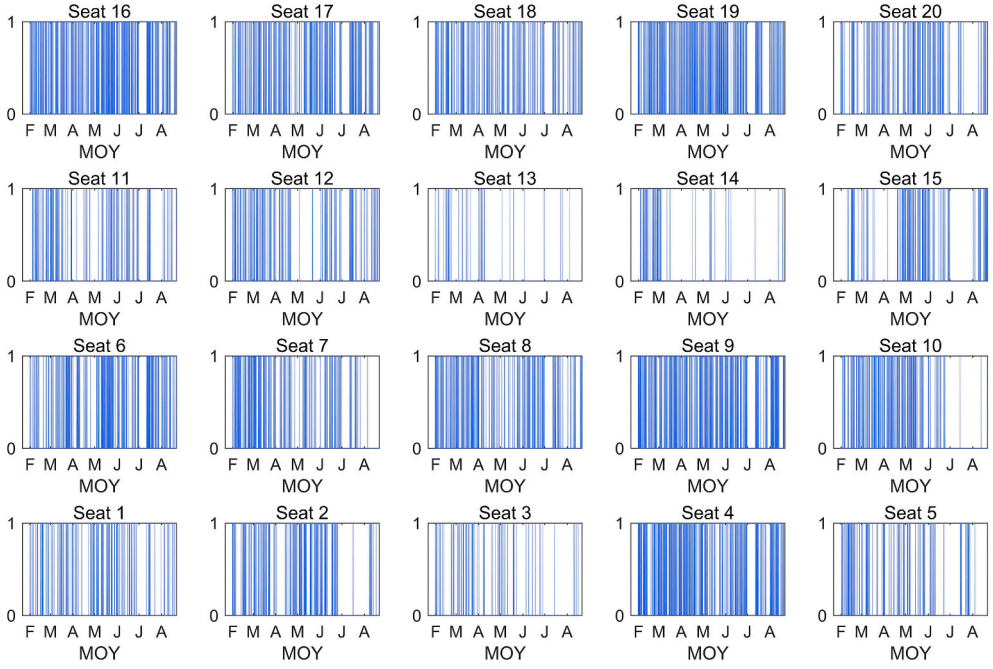

Fig. 3. Occupancy barcodes: chair-specific binary seated occupancy histories, $O_s(t)$, for each of the 20 desk-chair pairs from February 10 to August 31, 2019 visualized in the form of "occupancy barcodes." $O_s(t) = 0$ for seated absence and $O_s(t) = 1$ for seated presence. MOY = month of the year.

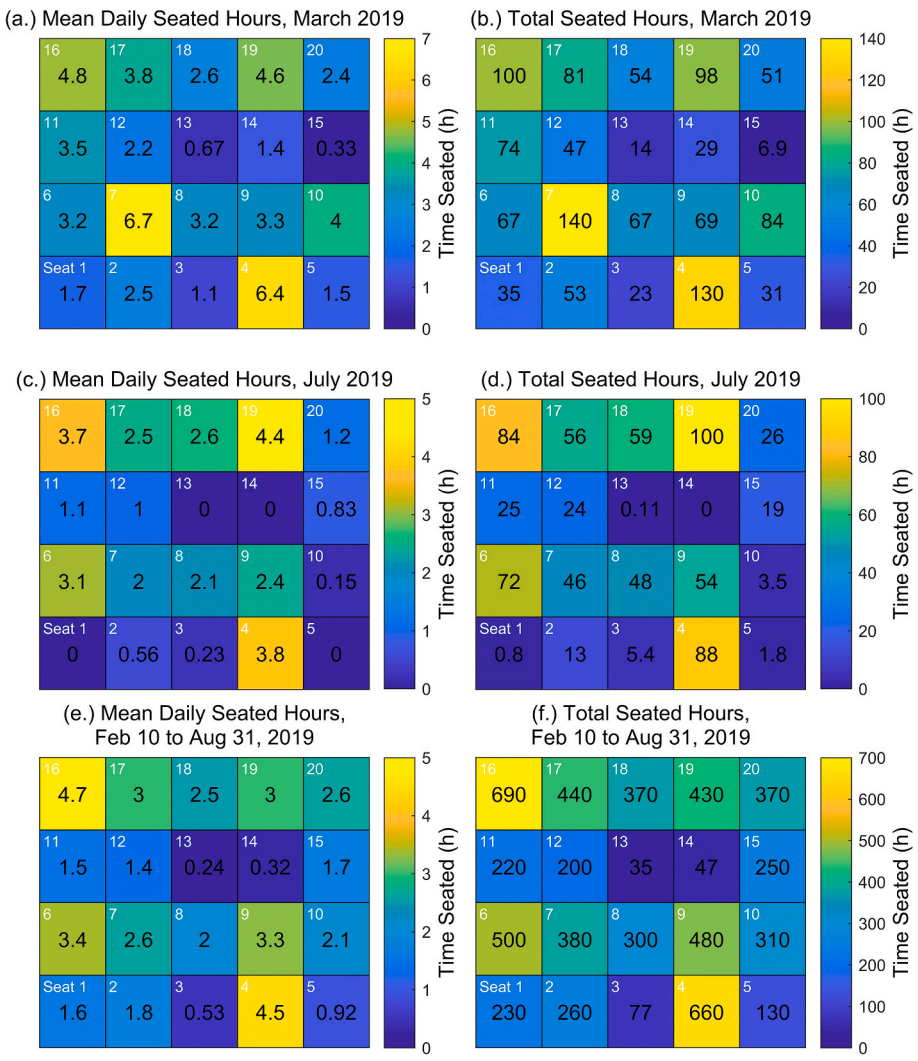

Fig. 4. Total seated hours, $\int O_s(t)\,dt$, for each desk-chair pair location: (a.) mean daily seated hours for weekdays in March 2019, (b.) total seated hours for March 2019, (c.) mean daily seated hours for weekdays in July 2019, (d.) total seated hours for July 2019, (e.) mean daily seated hours for weekdays from February 10 to August 31, 2019, and (f.) total seated hours from February 10 to August 31, 2019. Time seated (h) is denoted in each color bar. Values of zero were used to replace values that were < 0.1 h for the month. (For interpretation of the references to color in this figure legend, the reader is referred to the Web version of this article.)

fluctuations in $T_r(t)$ are minimal and temperatures generally remained in the range of 34–36 °C. Standing initiates an exponential decay in $T_r(t)$ back to $\overline{T}_m$. The temporal profiles of $T_m(t)$ and $T_r(t)$ shown in Fig. 2 are representative of those measured throughout the occupancy sensing campaign for all 20 chairs.

The sudden rise and decay in the seat surface temperature at the beginning and end of a seated occupancy period, respectively, demonstrates the temporal sensitivity in seated occupancy sensing with a chair-based temperature sensor array. This is due in part to rapid heat transfer via conduction between the occupant and chair-appended thermocouple that occurs when one sits on the cushion. As shown in Fig. 2, the moment when $T_r(t) > \overline{T}_m$, the $O_s(t)$ transitions step-wise from 0 (unoccupied chair) to 1 (occupied chair). Similarly, it can be seen that $O_s(t)$ transitions from 1 to 0 when $T_r(t)$ falls below 30 °C following the criteria established in Equation (2).

The seated occupancy profiles shown in Fig. 2 illustrate the stability of chair-based temperature sensing in monitoring continuous seated occupancy over extended periods (e.g. > 1 h) and in detecting transient periods of chair presence and absence. For example, in Fig. 2b between 16:00 and 19:00, two short unoccupied periods were observed to occur between longer, occupied periods. Negligible lag and high time-resolution suggest this approach can be suitable for integration with DCV and other HVAC&L control strategies for open-plan workspaces where prompt adjustments to the indoor environment are needed in response to individual, chair-specific occupancy changes.

3.3. Spatial seated occupancy trends determined via a chair-based temperature sensor array

The chair-based temperature sensor array enabled for evaluation of spatial seated occupancy trends in the Living Lab office over the 7-month measurement campaign (Figs. 3 and 4, and S1-S5). The chair-based temperature sensor array provides highly localized occupancy detection by monitoring the seated presence of an occupant at a known desk-chair pair location within the spatial grid of the open-plan office illustrated in Fig. 1. Chair-specific binary seated occupancy time-series, $O_s(t)$, and total seated hours over varying temporal scales, $\int O_s(t)\,dt$, are presented in Figs. 3 and 4, respectively. Both $O_s(t)$ and $\int O_s(t)\,dt$ are visualized in the same spatial grid as that of Fig. 1, with 4 rows of 5 seats each. For example, seat 13 is lateral to seats 12 and 14, and is also directly opposite to seat 18. Seats 5, 10, 15, and 20 are adjacent to a double-skin façade, and seats 1 and 6 are proximal to the entrance of the office space.

3.3.1. Occupancy barcodes: chair-specific binary seated occupancy histories

To demonstrate a unique application of the chair-based temperature sensor array, individual seated occupancy histories were calculated for each of the 20 desk-chair pairs and visualized in Fig. 3 in the form of "occupancy barcodes." Each of the 20 sub-plots in Fig. 3 presents the binary seated occupancy time-series, $O_s(t)$ (0–1), for each chair over 7

months. Each parallel vertical line indicates the beginning or end of a seated occupancy period, in the same manner as the $O_s(t)$ visualization presented for a single chair in Fig. 2b and d.

The spatial grid of 20 individual seated occupancy barcodes provides insights into month-to-month variations in chair-specific occupancy patterns for the open-plan office. Denser collections of vertical lines indicate more frequent seated presence at a given desk-chair pair location. Thus, the barcodes offer a useful visual tool for analyzing long-term, spatially-resolved fluctuations in seated occupancy for a shared indoor workspace. Barcodes for seats 4, 6, 9, 16, 17, and 19 reveal a pattern of frequent seated occupancy over 7 months. Conversely, barcodes for seats 3, 5, 13, and 14 display infrequent seated presence during the measurement campaign. Selected seats exhibit pronounced month-to-month variation in seated occupancy. For example, the barcode for seat 15 displays low seated occupancy from February to April, with a transition to more frequent seated occupancy between May and June. Similarly, the barcode for seat 12 reveals a sudden drop in seated occupancy in May, with more regular occupancy in adjacent months. Finer temporal gradients in seated occupancy can be observed in the barcodes. A gradual shift in seated presence in the barcode for seat 8 can be seen between April and May.

3.3.2. Spatial mapping of total seated hours per occupant

Integration of the chair-specific binary seated occupancy time-series, $O_s(t)$, presented in the occupancy barcodes provides temporally-resolved snapshots of total seated hours, $\int O_s(t)\,dt$, for each desk-chair pair location. Fig. 4 provides a spatial map of mean daily seated hours for weekdays and total seated hours for March 2019 (Fig. 4a and b), July 2019 (Fig. 4c and d), and for the entirety of the 7-month occupancy sensing campaign (Fig. 4e and f). Spatial maps for February, April, May, June, and August 2019 are provided in Figs. S1–S5. Mean daily and total seated hours for each desk-chair pair location are listed within each square of the spatial grid of the Living Lab office. The relationship between the color of each desk-chair pair location and time seated is shown in each color bar.

Spatial variations in time seated throughout the open-plan office can be observed in Fig. 4 and S1-S5. Desk-chair pairs with high seated occupancy are readily identified. For example, in March 2019, seats 4 and 7 (yellow/light orange squares) are associated with mean daily seated hours of 6.4 and 6.7 h, respectively, and total seated hours of 130 and 140 h, respectively; comparatively greater than other seats in the office. Likewise, seats with low to no seated occupancy can be quickly determined. In July 2019, seats 1, 3, 5, 10, 13, and 14 (dark blue squares) were found to have total monthly seated hours of less than 10 h.

The chair-based temperature sensor array offers a basis to monitor changes in spatially-resolved office usage schedules for individual occupants. Spatial variability in seated hours exhibits some month-to-month variation between February and August 2019 (Fig. 4 and S1-S5). This can be evaluated in part by considering the month-to-month variation in total seated hours for a given desk-chair pair. From February to August 2019, seat 4 transitions month-to-month from 57 to 130 to 140 to 72 to 82 to 88 to 85 h; and seat 20 varies month-to-month from 29 to 51 to 72 to 81 to 93 to 26 to 21 h.

The month-to-month variations in total seated hours presented in Fig. 4 and S1-S5 are consistent with the binary seated occupancy time-series shown in Fig. 3. The high density of vertical lines in the barcodes for seats 4, 6, 9, 16, 17, and 19 are associated with a greater number of total seated hours during the 7 month campaign: 660, 500, 480, 690, 440, and 430 h, respectively. Similarly, the infrequent seated occupancy presented in the barcodes for seats 3, 5, 13, and 14 are associated with the lowest number of total seated hours during the 7-month campaign: 77, 130, 35, and 47 h, respectively. The month-to-month variations shed light on differences in graduate student office attendance due to the academic semester structure for the spring, incorporating the months of February through mid-May 2019, and summer, incorporating the months of mid-May to mid-August 2019. In comparing March and July 2019 in Fig. 4, the open-plan office sees comparatively lower usage during the summer semester than the spring semester, with 16 out 20 seats showing a drop in seated presence. Figs. S1–S5 suggest that similar patterns in seated occupancy exist between the two semesters. Such differences can be explained by considering semesterly changes in course schedules, research activities, travel, and remote work. The insight gained from such variation patterns gives a general picture of the room usage throughout the year. Identifying these patterns in specific contexts can aid commercial management and decision-making in buildings to plan office space allocation and predict worker needs. Modern employment situations that allow employees to work remotely can save money by allocating a certain period of time for the offices to be open.

For the Living Lab office, there does not appear to be a meaningful relationship between seat location and seated occupancy frequency (Fig. 3) and total time seated (Fig. 4). Rather, seated presence is likely to depend on individual working schedules of the office occupants. In addition, there does not appear to be clustering of high or low occupancy seats adjacent to one another or along a given row or column of desks within the open-plan office grid.

3.4. Temporal seated occupancy trends determined via a chair-based temperature sensor array

The chair-based temperature sensor array enabled for evaluation of temporal trends in the total seated occupancy of the Living Lab office, $O_{s,total}(t)$, over the 7-month measurement campaign (Figs. 5–9). The binary seated occupancies for each of the 20 desk-chair pairs were summed to determine $O_{s,total}(t)$ with 15-s time resolution. Diurnal (Figs. 5–7) and weekly (Figs. 8–9) trends in $O_{s,total}(t)$ were characterized to demonstrate the usefulness of chair-based temperature sensing in monitoring occupancy profiles at the spatial-scale of the entire room.

The sampling period began towards the end of winter and continued through the spring and summer. Although the office air temperature profile remained relatively constant, the outdoor air temperatures varied from about −12 °C to 27 °C during this period [92]. Occupant clothes were not directly observed for the study; however, it can be assumed that clothing styles would vary seasonally. To explore the effect of seasonal clothing on the accuracy of the chair-based temperature sensor array, the median seat surface temperature was calculated for three occupants that showed similar relative occupancy levels throughout February, May, and August. The median temperatures for seats 9, 15, and 16 for occupied and unoccupied periods are shown in Table 1. From the colder to warmer months, there is a slight increase in occupied seat surface temperature, with less change in median temperature for unoccupied periods. Is likely that students wore relatively similar clothing while in the office, which may have varied with length and thickness; however the measurements were consistent in being able to detect seated presence across the seasons. This result confirms pilot tests done to explore the threshold of sensing. Pilot tests showed that adding layers and thick blankets to seats may delay the binary seated occupancy detection, as the seat temperature would rise more slowly.

3.4.1. Diurnal seated occupancy profiles in an open-plan office

Day-to-day variations in the diurnal total seated occupancy ($O_{s,total}(t)$) profile for the Living Lab office over 7 months is shown in Fig. 5. Each row illustrates the temporality in $O_{s,total}(t)$ (0.5 h average) for a given day of the year (DOY, 2019). The relationship between the color for a 0.5 h period and the total seated occupancy is shown in the color bar. The temporal map in $O_{s,total}(t)$ provides a basis to observe long-term trends in room-aggregated seated presence for an open-plan office. The white regions represent periods when seat surface temperature measurements were not conducted.

The chair-based temperature sensor array captured daily fluctuations

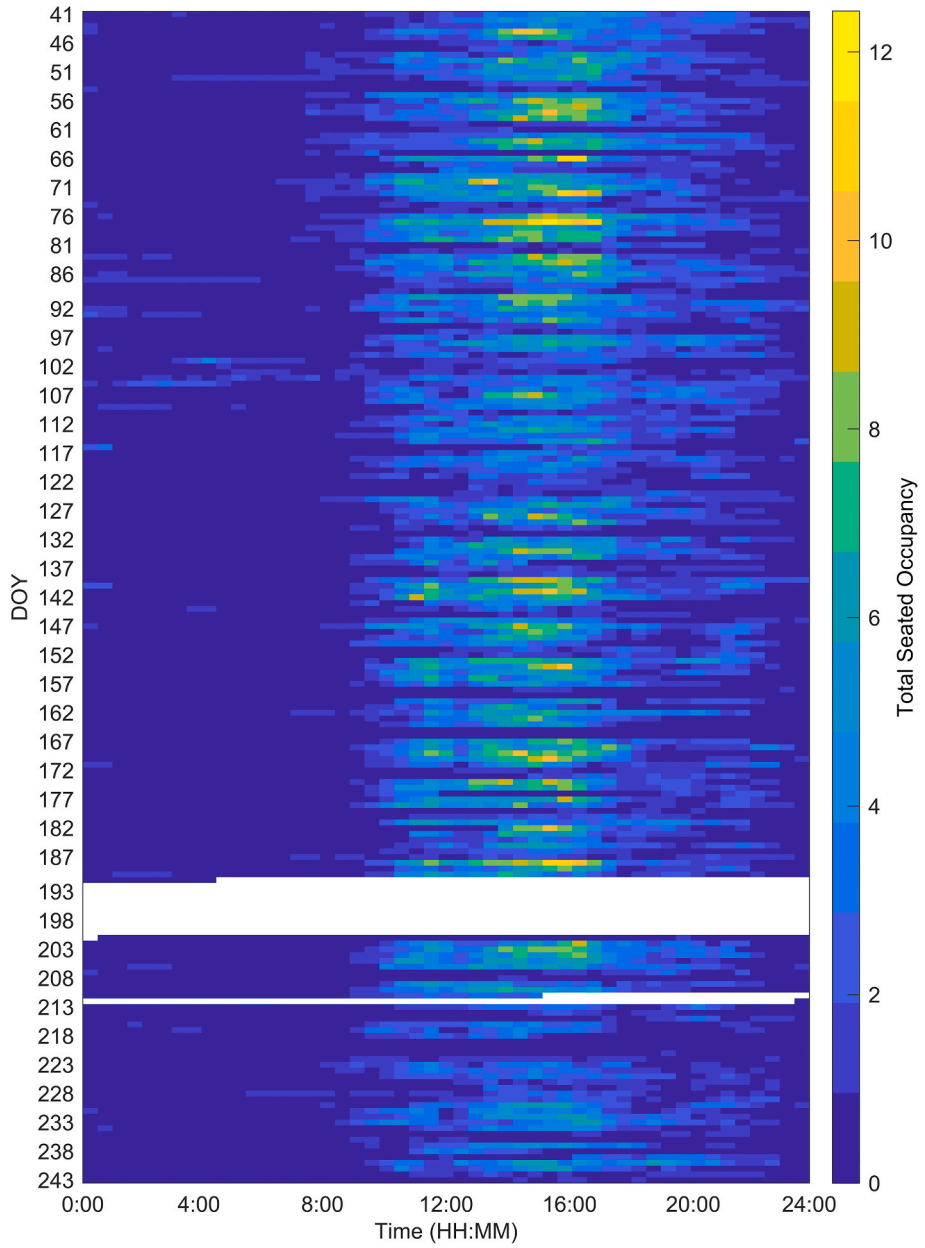

Fig. 5. Diurnal trends in the total seated occupancy, $O_{s,total}(t)$, from February 10 to August 31, 2019. $O_{s,total}(t)$ is denoted in the color bar. DOY = day of the year. White regions represent periods when seat surface temperature measurements were not conducted. (For interpretation of the references to color in this figure legend, the reader is referred to the Web version of this article.)

in the magnitude of the diurnal $O_{s,total}(t)$ profile throughout the measurement campaign (Fig. 5). From approximately DOY = 41 (February 10, 2019) to DOY = 90 (March 31, 2019) and from DOY = 138 (May 18, 2019) to DOY = 190 (July 09, 2019), $O_{s,total}(t)$ periodically reaches a maximum of 8–12 seated occupants (green/yellow/light orange bands) between 12:00 and 16:00. Conversely, from April to mid-May 2019 and in August 2019, the peak total seated occupancy in the afternoon was often less than 6 (cyan bands). Day-to-day variations in the magnitude of $O_{s,total}(t)$ were less common in the late afternoon and evening (16:00 to 24:00) and during the early morning (00:00 to 10:00). During these periods, $O_{s,total}(t)$ generally remained below 2 (dark blue bands). Day-to-day variations in $O_{s,total}(t)$ shown in Fig. 5 are consistent with the temporal variations in $O_s(t)$ observed in Fig. 3.

Similarities in the shape of the diurnal $O_{s,total}(t)$ profile can be observed in Fig. 5. Total seated occupancy in the Living Lab office nearly always reached its peak between the hours of 12:00 to 16:00, irrespective of the day of the week (weekday or weekend), week, or month. This peak in $O_{s,total}(t)$ during the afternoon can be readily observed by following the incremental increase in $O_{s,total}(t)$ (transition in color gradient) from morning to afternoon to evening. It can be seen that the shape of the diurnal $O_{s,total}(t)$ profile remains flat at, or close to, 0 (dark blue) during the non-traditional work periods in the late evening/early morning hours of 23:00 to 08:00. As illustrated in Fig. 5, monitoring long-term trends in the diurnal $O_{s,total}(t)$ profile with chair-appended thermocouples provides a basis to understand how the room-aggregated usage profiles of a collaborative open-plan office environment change over varying time-scales.

Diurnal trends in $O_{s,total}(t)$ for each DOY were aggregated to calculate mean and median characteristic seated occupancy profiles with 15-s time resolution for the office for weekdays (Monday to Friday) and weekends (Saturday and Sunday) during the spring (February 10 to April 31, 2019) and summer (May 01 to August 31, 2019) academic

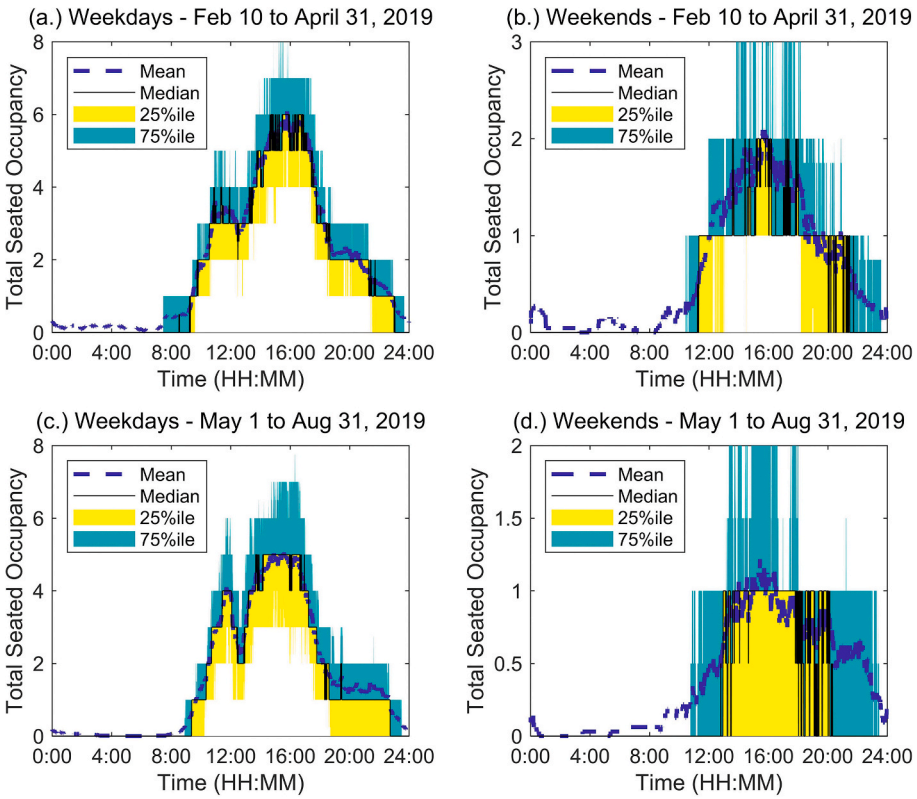

Fig. 6. Characteristic total seated occupancy profiles, $O_{s,total}(t)$, for: (a.) weekdays from February 10 to April 31, 2019, (b.) weekends from February 10 to April 31, 2019, (c.) weekdays from May 01 to August 31, 2019, (d.) weekends from May 01 to August 31, 2019. The dashed blue lines indicate the mean $O_{s,total}(t)$, the solid black lines indicate the median $O_{s,total}(t)$, and the yellow and green lines indicate the 25th and 75th percentiles, respectively. (For interpretation of the references to color in this figure legend, the reader is referred to the Web version of this article.)

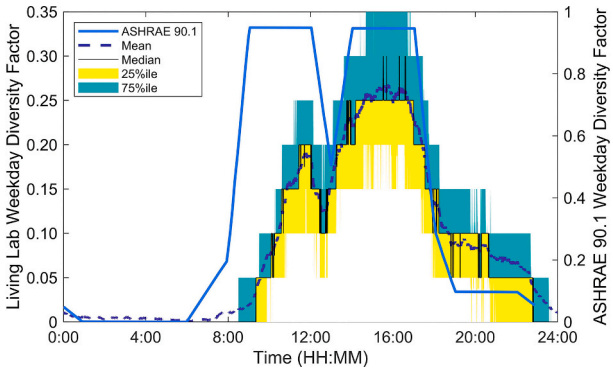

Fig. 7. Weekday occupancy diversity factors: Living Lab seated occupancy diversity factor for a room capacity of 20 seats (left y-axis) and occupancy diversity factor following ASHRAE 90.1 (right y-axis, via [70]). For the Living Lab diversity factor: the dashed blue lines indicate the mean, the solid black lines indicate the median, and the yellow and green lines indicate the 25th and 75th percentiles, respectively. (For interpretation of the references to color in this figure legend, the reader is referred to the Web version of this article.)

semesters (Fig. 6). The dashed blue lines indicate the mean $O_{s,total}(t)$, the solid black lines indicate the median $O_{s,total}(t)$, and the yellow and green lines indicate the 25th and 75th percentiles, respectively. The characteristic profiles in total seated occupancy are unique to the Living Lab office, where graduate students follow flexible and course- and research-dependent work schedules. Total seated occupancy trends observed for this office confirm that different contexts can shift the times and magnitudes that people are present in a such an indoor space.

The characteristic diurnal $O_{s,total}(t)$ profiles (both mean and median) for weekdays (Fig. 6a and c) exhibit a trimodal shape, with a prominent peak in room occupancy at around 16:00 and secondary peaks at around 12:00 and 20:00. The prominent peak varies between $O_{s,total}(t) =$ 4 to 7 during the spring semester, with a mean and median of approximately $O_{s,total}(t) =$ 5–6; and between $O_{s,total}(t) = 3$ to 7 during the summer semester, with a mean and median of approximately $O_{s,total}(t) =$ 4–5. The secondary peak at around 12:00 is preceded by a gradual buildup in total seated occupancy at a rate of approximately 1 additional seated occupant per hour. Between 12:00 and 13:00, $O_{s,total}(t)$ drops by about 1 during the spring semester and about 2 during the summer semester. From 13:00 to 16:00, the totaled seated occupancy gradually grows to the prominent peak, where it then follows a downward trend at a rate of roughly 0.6 to 0.7 seated occupants per hour to near 0 at 24:00. However, a small bump in seated occupancy can be seen at 20:00. The variation (25th to 75th percentile) in the weekday $O_{s,total}(t)$ is typically $\pm$ 1 seated occupant about the median between 08:00 to 14:00 and 17:00 to 24:00, and $\pm$1 to 2 seated occupants about the median from 14:00 to 16:00. The temporal variation in $O_{s,total}(t)$ during the weekdays is consistent with the day-to-day fluctuations in $O_{s,total}(t)$ observed in Fig. 5.

The characteristic diurnal $O_{s,total}(t)$ profiles (both mean and median) for weekends (Fig. 6b and d) exhibit a unimodal shape, with a prominent peak at around 16:00. During the spring semester, the magnitude of the prominent peak is approximately $O_{s,total}(t) = 2$ and during the summer semester, the magnitude tapers off to roughly $O_{s,total}(t) = 1$. It is evident that the Living Lab office is consistently emptier during the weekends compared to the weekdays.

3.4.2. *Weekly seated occupancy profiles in an open-plan office*

Weekly total seated occupancy ($O_{s,total}(t)$) profiles (Monday through Sunday) for the Living Lab office over 7 months are shown in Fig. 8. Similar to Fig. 5, each row illustrates the temporality in $O_{s,total}(t)$ (0.5 h average) for a given week of the year (WOY, 2019). The relationship between the color for a 0.5 h period and the total seated occupancy is shown in the color bar. The white regions represent periods when seat surface temperature measurements were not conducted. Fig. 8 offers an alternative visualization of temporal trends in the total seated occupancy as compared to Figs. 5 and 6 and provide a basis to observe of how

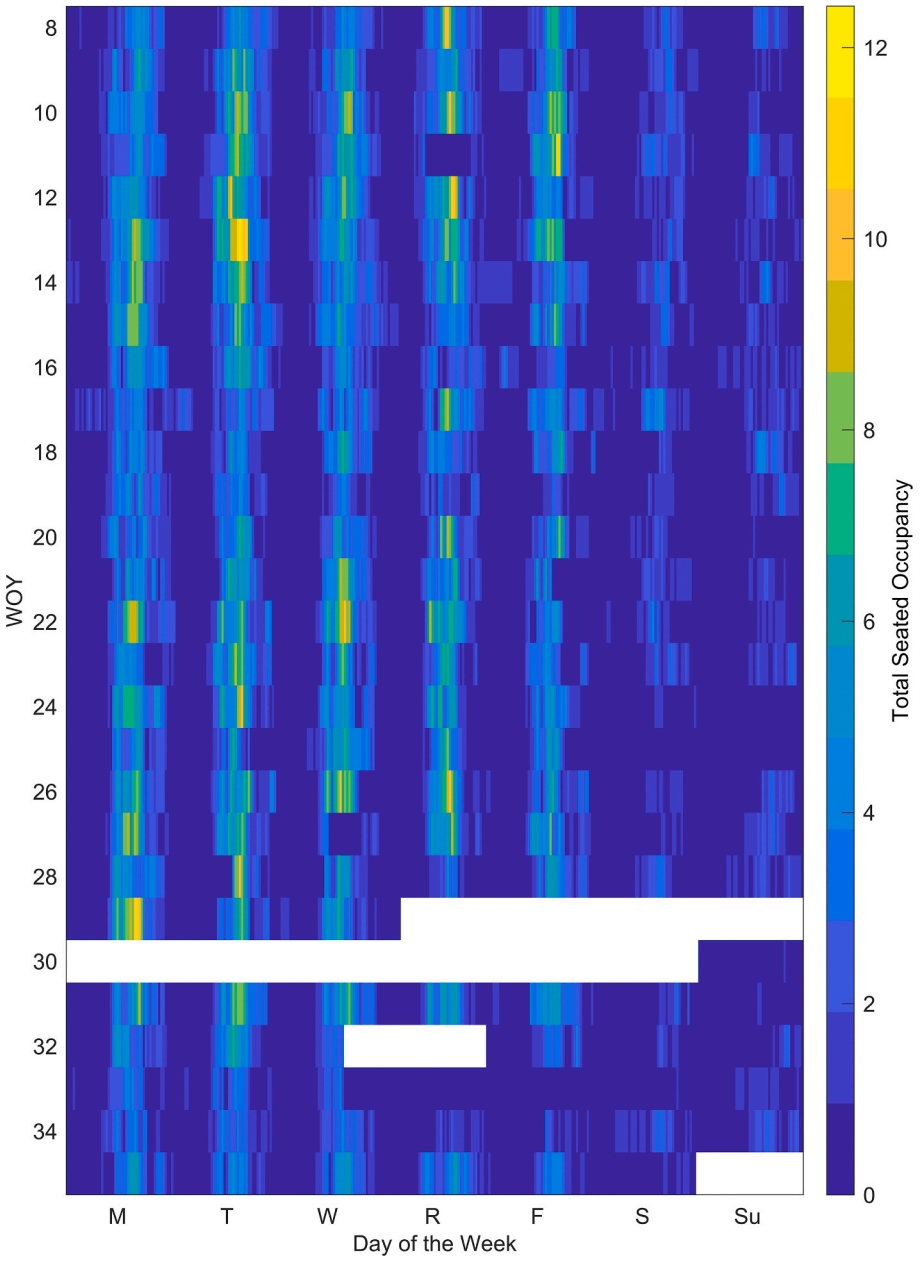

Fig. 8. Weekly trends in the total seated occupancy, $O_{s,total}(t)$, from February 10 to August 31, 2019. $O_{s,total}(t)$ is denoted in the color bar. WOY = week of the year. White regions represent periods when seat surface temperature measurements were not conducted. (For interpretation of the references to color in this figure legend, the reader is referred to the Web version of this article.)

occupancy changes with the day of the week.

Month-to-month and semesterly variations in the weekly $O_{s,total}(t)$ profile can be seen in Fig. 8, mirroring those observed for $O_s(t)$ and $\int O_s(t)\,dt$ in Figs. 3, 4, and S1-S5. Bands of elevated total seated occupancy (green/yellow/light orange) can be seen between Monday through Friday. In general, periods when $O_{s,total}(t) > 10$ are less common on Friday compared to Monday through Thursday. The diurnal trend in $O_{s,total}(t)$ for a given day of the week is relatively consistent during the 7-month measurement campaign, however, some variability can be seen on Saturday and Sunday due to the more inconsistent work schedules on the weekends (see Fig. 6).

3.4.3. *Categorization of seated occupancy by relative presence*

As the chair-based temperature sensor array monitors seated occupancy histories for each desk-chair pair, individual occupancy trends ($O_s(t)$, Fig. 3) can be compared to the aggregated whole ($O_{s,total}(t)$, Figs. 5 and 8). While diurnal and weekly trends in $O_{s,total}(t)$ are most commonly reported for office environments, such room-scale occupancy profiles do not account for the unique seated occupancy schedules of each office occupant. It is evident through the individual seated occupancy barcodes displayed in Fig. 3 that each desk-chair pair is occupied in varying amounts, with some seats occupied significantly more (e.g. seats 16 and 17) than others (e.g. seats 13 and 14). As discussed in Section 3.1, each chair was ranked as high, medium, or low according to the amount of time they were employed relative to the other seats, where $n = 4$ desk-chair pairs were ranked as high, $n = 5$ chairs were ranked as medium, and $n = 11$ as low.

Fig. 9 presents the weekly profile (Monday through Sunday) in the seated occupancy probability for each category of relative presence (high: yellow, medium: cyan, and low: violet). The occupancy probability ranges from 0, where the likelihood of seated occupancy is null at a particular time, to 1, where the likelihood of seated occupancy is certain

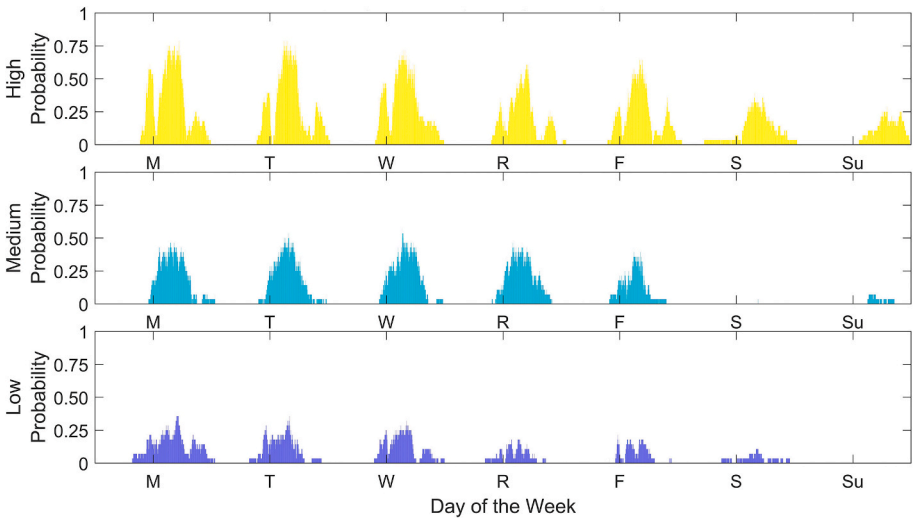

Fig. 9. Weekly trends in the seated occupancy probability for each category of relative presence: high (top), medium (middle), and low (bottom). The occupancy probability ranges from 0, where the likelihood of seated occupancy is null at a particular time, to 1, where the likelihood of seated occupancy is certain at a particular time.

Table 1
Median seat surface temperatures for three desk-chair pairs during occupied and unoccupied periods.

Seat No.	February Median (°C)		May Median (°C)		August Median (°C)	
	Occupied	Unoccupied	Occupied	Unoccupied	Occupied	Unoccupied
9	33.1	21.9	35.5	23.5	35.5	23.5
15	33.6	22.2	34.0	22.0	34.0	22.5
16	31.9	22.5	34.0	22.0	34.0	22.0

at a particular time. Fig. 9 demonstrates how measuring chair-specific seated occupancy with a chair-based temperature sensor array can be used to cluster occupants based on relative time spent in the office, providing an extra layer of information beyond aggregated $O_{s,total}(t)$ profiles. The temporal profiles in Fig. 9 can be interpreted as the probability of a seat in one of the categories as being occupied at a certain time, however a larger sample size or context-dependent measurements would be needed to more accurately represent other settings.

Different diurnal and weekly seated occupancy trends emerge among the three categories of seated presence. The weekday diurnal seat occupancy probabilities for the high occupancy desk-chair pairs show a trimodal shape with three distinct peaks at approximately 12:00, 16:00, and 20:00. The medium seats are primarily unimodal in shape during the weekdays and the low seats have a less defined shape. The high category seats have occupancy probabilities reaching and exceeding 0.50 during peak hours, whereas the medium category seats are likely to be occupied less than 50% of the time during weekday afternoons. Low category seats are much less likely to be occupied, with probabilities less than 0.25.

All three categories show stronger seated presence during the weekdays, especially Monday through Wednesday, followed by a noticeable decrease on Thursday and Friday, and additional reduction on the weekend. The seats in the low occupancy category are occupied throughout the week in a seemingly unpredictable pattern, suggesting irregular use patterns of the Living Lab office. Conversely, seats in the high occupancy category follow a more recurrent office use schedule. Weekday occupancy probability distributions shown by Peng et al. (2017) yielded multi-person offices with notable bimodal distributions and several personal offices with less predictable schedules [30], similar to the low occupancy category for the Living Lab office. The offices studied in Ref. [30] also showed higher variety than multi-person offices for different days of the week.

4. Discussion

4.1. Applications of spatial seated occupancy detection in an open-plan office

Monitoring the seated presence of individual occupants with chair-appended thermocouples, rather than the composite office population as is done with delocalized occupancy sensing techniques (e.g. a single CO_2 or door PIR sensor per office), allows for the creation of a spatial grid of office use schedules over varying time scales (Figs. 3 and 4). Such spatial patterns can inform the regularity, or irregularity, of office occupancy among specific occupants or groups of occupants. Chair-resolved seated occupancy data can identify hourly, daily, weekly, and monthly trends in an individual's use of a shared workspace. The high degree of variability observed in both $O_s(t)$ and $\int O_s(t)\,dt$ among the 20 desk-chair pairs in the Living Lab office suggest the need for monitoring individual occupancy trends in a modern open-plan office environment.

The creation of spatial maps of $O_s(t)$ and $\int O_s(t)\,dt$ enabled by the deployment of a chair-based temperature sensor array provides a basis to infer how chair-specific seated occupancy trends influence indoor environmental quality in a collaborative open-plan office. Tracking the historical presence of people seated in a room (Fig. 3) is useful for studying the long-term impact of thermal comfort, lighting, ventilation, and indoor air quality on productivity and health. Binary seated occupancy time-series can be integrated with material balance models and per person emission rates to estimate concentrations of human-associated species, such as biological particles and VOCs. Individual occupancy trends can inform the contribution of a given occupant to the total concentration of a particular species.

The spatial maps of $O_s(t)$ can be used with computational fluid dynamics simulations to model the spatial dispersion of human-associated species and subsequent inhalation exposure of seated receptors at varying distances from the seated source. Spatially-resolved tracking of

seated occupants is especially of value in understanding airborne transmission of viruses produced by respiratory activities. Furthermore, spatial indoor seated occupancy monitoring platforms based on chair-based temperature sensing can be integrated with contact tracing during pandemics to reduce the spread of infectious diseases. Spatial maps in $O_s(t)$ and $\int O_s(t)\,dt$ can guide open-plan office seat assignments to decrease the likelihood that people are in close spatial proximity to one another by considering individual office use patterns.

4.2. Diurnal seated occupancy diversity factor profiles

The diurnal profiles in total seated occupancy determined by the chair-based temperature sensor array (Figs. 5 and 6) can be used to evaluate a time-resolved seated occupancy diversity factor following ANSI/ASHRAE/IES Standard 90.1–2019. When a room's utilization schedule is not known, ASHRAE 90.1 suggests using an occupancy diversity factor based on predicted office demand for weekdays and weekends. As such, diversity factors are of value for conducting energy simulations for office environments under variable occupancy [70]. The occupancy diversity factor can be determined by dividing the actual room occupancy by the room seat capacity and thus, ranges from 0 for an unoccupied room to 1 for a room occupied at capacity. Fig. 7 illustrates the weekday seated occupancy diversity factor computed for the Living Lab office with a room capacity of 20 seats (left y-axis: mean, median, and 25th/75th percentile for February 10 to August 31, 2019) and the weekday office occupancy diversity factor recommended by ASHRAE 90.1 (right y-axis) [70].

The Living Lab and ASHRAE 90.1 weekday occupancy diversity factors are similar in shape, yet different in magnitude. As discussed previously, the characteristic weekday diurnal $O_{s,total}(t)$ profile exhibits two peaks at around 12:00 and 16:00. Each peak in $O_{s,total}(t)$ corresponds to a peak in the seated occupancy diversity factor, which is approximately 0.20 at 12:00 and 0.25 at 16:00. At 16:00, the diversity factor varies been 0.15 (25th percentile) and 0.35 (75th percentile), demonstrating that the Living Lab room occupancy commonly remains below one-third of its 20 seat capacity. The ASHRAE 90.1 occupancy diversity factor shows step-wise peaks at approximately the same time intervals as for the Living Lab office. However, the magnitude of the ASHRAE 90.1 occupancy diversity factor is much greater, with peaks approaching 1 from 09:00 to 12:00 and 14:00 to 17:00. During the evening, from 19:00 to 22:00, the Living Lab and ASHRAE 90.1 diversity factors are more similar in magnitude, varying between 0.075 and 0.10. The differences observed between the Living Lab and ASHRAE 90.1 diversity factors highlight the potential benefits that can be gained by tailoring building demand to specific office environments [70], especially for offices such as the Living Lab which operate under atypical workday schedules.

Classifying a room based on fullness and the diversity of work-related activities helps to understand the energy demand with regards to lighting, electronic devices, heating and cooling, and ventilation. Similar to this study, Duarte et al. (2013) compared monthly measured room occupancies in commercial offices to the ASHRAE 90.1 diversity factor schedule [70]. Both private and open-plan offices had notable overlap with the peak times of energy demand, but differed notably in peak magnitudes, which were overestimated by the ASHRAE 90.1 diversity factor. This difference was exacerbated on days on or near holidays and was also variable for different spaces and days of the week.

4.3. Seated occupancy sensing considerations and limitations

Occupant sensing campaigns must consider indoor space usage to select accurate sensing systems. The chair-based thermocouple arrays introduced in this study are evaluated as accurate for estimating seated occupancy. When someone sits in a chair, provided the chair is not heavily covered in layers of thick blankets or jackets, the datalogger instantly senses one's presence. The algorithm used to estimate occupancy after data collection ensures that the binary occupancy is noted within 15 s of the real action. This method has an advantage over other seat-based occupancy measurement systems in that thermal sensing tailors to human detection, while pressure detection may add false-positives [90]. As it is an instantaneous method of seated occupancy sensing, it does not require training for post-occupancy estimations; however, methods of real-time data collection would further the application potential of the thermocouple arrays. Because 20 separate sensors and dataloggers were used to create an array detection system, of known locations, the spatial grid reflects exact desk locations. Device-centered detection methods such as a Bluetooth and WiFi sensing can also be used to create a grid using sensors, and can detect zone-based location, rather than exact occupant location [73,77].

In order to capture the presence of standing or moving individuals in a space intended for primarily sitting, a seated occupancy detection method can be combined with room-based sensors, such as PIR or cameras. Delocalized occupancy sensing in larger buildings with more frequent room traversal, rather than smaller zones, is possible with the use of less accurate, but more broader sensing techniques, including Bluetooth, WiFi, and PIR, rather than seat-based sensors.

5. Conclusions

This study developed and evaluated a novel indoor occupancy sensing technique – a chair-based temperature sensor array – to monitor seated occupancy patterns in an open-plan office environment. The chair-based temperature sensor array enabled for highly localized seated occupancy detection by tracking the seat surface temperatures and binary seated occupancies of each chair in the office with 15-s time resolution. The technique offers advantages compared to delocalized occupancy sensing techniques, such as a single CO_2 or door PIR sensor per office. Notably, spatial maps in chair-specific seated occupancy trends over varying temporal scales offer insight into how each occupant contributes to office energy expenditures. The near-instant rise and decay in seat surface temperatures at the beginning and end of a seated period, respectively, demonstrates that this non-invasive technique can rapidly detect seated presence. Chair-based temperature sensing provides a means to categorize seated occupancy by relative level of presence in the office and cluster occupants by the amount of time they spend in a modern, collaborative indoor workspace. This technique is well suited for indoor environments that are primarily used for sitting-related tasks in a single, well-defined zone.

The chair-based temperature sensor array captures the diversity in office use patterns for populations that do not follow traditional work schedules. In societies fueled more by service- and technology-based industries, the idea of a typical office setting is becoming more abstract as buildings get creative with flexible definitions for office environments. Development of co-working spaces, the ability to work from home, and on-demand workplaces attract companies and freelancers alike, with the opportunities to save costs, promote creative collaboration, and reduce air pollution due to unnecessary commutes [93]. Straying from the traditional 09:00 to 17:00 workday will have drastic effects on predicted building usage profiles and the resulting temporal energy demands. Proper energy audits and smart buildings can help to avert avoidable energy spending in these unique contexts. As shown in this study for a Living Lab office, seated occupancy profiles vary considerably among the 20 occupants due the flexible work schedules of the graduate students.

Seated occupancy monitoring with chair-appended thermocouples can guide research on how people shape the composition of indoor air as individual occupancy profiles are continually recorded. The chair-based temperature sensor array can be used streamline data collection for epidemiology studies to monitor the continuity and extent of time individuals spend sitting continuously at work. Reliable, continuous monitoring can aid in improving sitting-related information in specific environments and can be used to tailor intervention strategies to prevent

sedentary-related health problems, such as encouraging management to allow for more active workplaces [49]. A low-cost, flexible version of the thermocouple setup could relay information to an app that tells people how long they are present, allowing them to track their own office time as well as levels of continuous sitting.

Future efforts can focus on integration of a chair-based temperature sensor array with IoT-based platforms for buildings. Real-time data coordination through wireless connectivity would reduce the need for manual downloading of seat surface temperatures. Chair-based occupancy detection methods resulting from novel uses of sensors and controllers can be upscaled for applications where people sit most of the time, such as in offices, classrooms, auditoriums, and in transportation. As many large-scale, multi- and single-tenant office buildings currently use CO_2-based DCV, these HVAC&L strategies can be improved when integrated with seat-based sensors that immediately detect the number of occupants to decrease lag and occupant schedule uncertainties. While this thermocouple setup detects seated occupant locations with a high degree of accuracy, the next step in delivering location-based HVAC&L control, whether for thermal comfort or energy efficiency, depends on the capabilities of the HVAC&L system itself to deliver tailored responses. Even with dependable monitoring is it also important to consider that quantitative occupancy detection is not a substitute for qualitative information, such as desired occupant preferences of thermal status or activity levels [49]. Horr et al. (2016) conclude in a review of indoor environmental quality and occupants that sensors related to building systems could increase productivity by automatically relaying subjective feedback information to companies to tailor the building to employees [50].

Declaration of competing interest

The authors declare that they have no conflict of interest.

Acknowledgements

Financial support was provided by the National Science Foundation (CBET-1805804 and CBET-1847493) and an American Society of Heating, Refrigerating, and Air Conditioning Engineers Graduate Student Grant-In-Aid Award (to DNW). The authors would like to thank the staff at the Ray W. Herrick Laboratories for facilitating the work for this project.

Appendix A. Supplementary data

Supplementary data to this article can be found online at https://doi.org/10.1016/j.buildenv.2020.107360.

References

[1] A. Feige, H. Wallbaum, M. Janser, L. Windlinger, "Impact of sustainable office buildings on occupant's comfort and productivity, J. Corp. R. Estate 15 (1) (Mar. 2013) 7–34, https://doi.org/10.1108/JCRE-01-2013-0004.
[2] N. Li, G. Calis, B. Becerik-Gerber, Measuring and monitoring occupancy with an RFID based system for demand-driven HVAC operations, Autom. ConStruct. 24 (Jul. 2012) 89–99, https://doi.org/10.1016/j.autcon.2012.02.013.
[3] J. Joe, P. Karava, X. Hou, Y. Xiao, J. Hu, A distributed approach to model-predictive control of radiant comfort delivery systems in office spaces with localized thermal environments, Energy Build. 175 (Sep. 2018) 173–188, https://doi.org/10.1016/j.enbuild.2018.06.068.
[4] F. Weikl, et al., Fungal and bacterial communities in indoor dust follow different environmental determinants, PloS One 11 (4) (Apr. 2016), e0154131, https://doi.org/10.1371/journal.pone.0154131.
[5] M.S. Alshitawi, H.B. Awbi, "Measurement and prediction of the effect of students' activities on airborne particulate concentration in a classroom, HVAC R Res. 17 (4) (Aug. 2011) 446–464, https://doi.org/10.1080/10789669.2011.583708.
[6] D. Hospodsky, et al., Human occupancy as a source of indoor airborne bacteria, PloS One 7 (4) (Apr. 2012), e34867, https://doi.org/10.1371/journal.pone.0034867.
[7] P. Mochalski, J. King, K. Unterkofler, H. Hinterhuber, A. Amann, Emission rates of selected volatile organic compounds from skin of healthy volunteers, J. Chromatogr. B 959 (May 2014) 62–70, https://doi.org/10.1016/j.jchromb.2014.04.006.
[8] D. Licina, W.W. Nazaroff, Clothing as a transport vector for airborne particles: chamber study, Indoor Air 28 (3) (May 2018) 404–414, https://doi.org/10.1111/ina.12452.
[9] K. Weekly, D. Rim, L. Zhang, A.M. Bayen, W.W. Nazaroff, C.J. Spanos, Low-cost coarse airborne particulate matter sensing for indoor occupancy detection, in: 2013 IEEE International Conference on Automation Science and Engineering (CASE), Madison, WI, USA, 2013, pp. 32–37, https://doi.org/10.1109/CoASE.2013.6653970.
[10] Y. Jeon, et al., IoT-based occupancy detection system in indoor residential environments, Build. Environ. 132 (Mar. 2018) 181–204, https://doi.org/10.1016/j.buildenv.2018.01.043.
[11] T. Wu, et al., Infant and adult inhalation exposure to resuspended biological particulate matter, Environ. Sci. Technol. 52 (1) (Jan. 2018) 237–247, https://doi.org/10.1021/acs.est.7b04183.
[12] A.W. Nørgaard, J.D. Kudal, V. Kofoed-Sørensen, I.K. Koponen, P. Wolkoff, Ozone-initiated VOC and particle emissions from a cleaning agent and an air freshener: risk assessment of acute airway effects, Environ. Int. 68 (Jul. 2014) 209–218, https://doi.org/10.1016/j.envint.2014.03.029.
[13] R. Castorina, et al., Volatile organic compound emissions from markers used in preschools, schools, and homes, Int. J. Environ. Anal. Chem. 96 (13) (Oct. 2016) 1247–1263, https://doi.org/10.1080/03067319.2016.1250892.
[14] T.C. Wang, A study of bioeffluents in a college classroom, Build. Eng. 87 (1) (1975).
[15] M.A.G. Wallace, J.D. Pleil, M.C. Madden, Identifying organic compounds in exhaled breath aerosol: non-invasive sampling from respirator surfaces and disposable hospital masks, J. Aerosol Sci. 137 (Nov. 2019), 105444, https://doi.org/10.1016/j.jaerosci.2019.105444.
[16] A. Amann, et al., The human volatilome: volatile organic compounds (VOCs) in exhaled breath, skin emanations, urine, feces and saliva, J. Breath Res. 8 (3) (Jun. 2014), 034001, https://doi.org/10.1088/1752-7155/8/3/034001.
[17] X. Tang, P.K. Misztal, W.W. Nazaroff, A.H. Goldstein, Volatile organic compound emissions from humans indoors, Environ. Sci. Technol. 50 (23) (Dec. 2016) 12686–12694, https://doi.org/10.1021/acs.est.6b04415.
[18] C. Yeretzian, A. Jordan, W. Lindinger, Analysing the headspace of coffee by proton-transfer-reaction mass-spectrometry, Int. J. Mass Spectrom. (Jan. 2003) 115–139, https://doi.org/10.1016/S1387-3806(02)00785-6, 223–224.
[19] J. Xiong, Z. He, X. Tang, P.K. Misztal, A.H. Goldstein, Modeling the time-dependent concentrations of primary and secondary reaction products of ozone with squalene in a university classroom, Environ. Sci. Technol. 53 (14) (Jul. 2019) 8262–8270, https://doi.org/10.1021/acs.est.9b02302.
[20] S. Liu, et al., Contribution of human-related sources to indoor volatile organic compounds in a university classroom, Indoor Air 26 (6) (Dec. 2016) 925–938, https://doi.org/10.1111/ina.12272.
[21] J. Qian, D. Hospodsky, N. Yamamoto, W.W. Nazaroff, J. Peccia, Size-resolved emission rates of airborne bacteria and fungi in an occupied classroom: size-resolved bioaerosol emission rates, Indoor Air 22 (4) (Aug. 2012) 339–351, https://doi.org/10.1111/j.1600-0668.2012.00769.x.
[22] C. Stönner, et al., Proof of concept study: testing human volatile organic compounds as tools for age classification of films, PloS One 13 (10) (Oct. 2018), e0203044, https://doi.org/10.1371/journal.pone.0203044.
[23] P. Wolkoff, Impact of air velocity, temperature, humidity, and air on long-term voc emissions from building products, Atmos. Environ. 32 (14–15) (Aug. 1998) 2659–2668, https://doi.org/10.1016/S1352-2310(97)00402-0.
[24] M. Callesen, et al., Associations between selected allergens, phthalates, nicotine, polycyclic aromatic hydrocarbons, and bedroom ventilation and clinically confirmed asthma, rhinoconjunctivitis, and atopic dermatitis in preschool children, Indoor Air 24 (2) (Apr. 2014) 136–147, https://doi.org/10.1111/ina.12060.
[25] X. Zhang, P. Wargocki, Z. Lian, C. Thyregod, Effects of exposure to carbon dioxide and bioeffluents on perceived air quality, self-assessed acute health symptoms, and cognitive performance, Indoor Air 27 (1) (Jan. 2017) 47–64, https://doi.org/10.1111/ina.12284.
[26] U. Satish, et al., Is CO_2 an indoor pollutant? Direct effects of low-to-moderate CO_2 concentrations on human decision-making performance, Environ. Health Perspect. 120 (12) (Dec. 2012) 1671–1677, https://doi.org/10.1289/ehp.1104789.
[27] "Ventilation for Acceptable Air Quality," *ANSI/ASHRAE Addendum P to ANSI/ASHRAE Standard 62.1-2013*, July 2015.
[28] M.G. Apte, "A Review of Demand Control Ventilation," *LBNL-60170 Report*, May 2006.
[29] Z.D. O'Neill, Y. Li, H.C. Cheng, X. Zhou, S.T. Taylor, "Energy Savings and Ventilation Performance from CO $_2$ -based Demand Controlled Ventilation: Simulation Results from ASHRAE RP-1747 (ASHRAE RP-1747)," *Science and Technology for the Built Environment*, Jun. 2019, pp. 1–25, https://doi.org/10.1080/23744731.2019.1620575.
[30] Y. Peng, A. Rysanek, Z. Nagy, A. Schlüter, Occupancy learning-based demand-driven cooling control for office spaces, Build. Environ. 122 (Sep. 2017) 145–160, https://doi.org/10.1016/j.buildenv.2017.06.010.
[31] F. Oldewurtel, D. Sturzenegger, M. Morari, Importance of occupancy information for building climate control, Appl. Energy 101 (Jan. 2013) 521–532, https://doi.org/10.1016/j.apenergy.2012.06.014.
[32] L. Nikdel, K. Janoyan, S.D. Bird, S.E. Powers, Multiple perspectives of the value of occupancy-based HVAC control systems, Build. Environ. 129 (Feb. 2018) 15–25, https://doi.org/10.1016/j.buildenv.2017.11.039.
[33] P. Carreira, A.A. Costa, V. Mansur, A. Arsénio, Can HVAC really learn from users? A simulation-based study on the effectiveness of voting for comfort and energy use

optimization, Sustain. Cities Soc. 41 (Aug. 2018) 275–285, https://doi.org/10.1016/j.scs.2018.05.043.
[34] M. Shehadi, Occupancy Detection Chair Sensor: an Energy Conservation Tool, vol. 13, *American Society for Engineering Education Conference & Exposition*, 2018.
[35] J.Y. Park, T. Dougherty, Z.N. Intelligent, "A Bluetooth Based Occupancy Detection for Buildings," *Building Performance Modeling Conference and SimBuild*, Co-organized by ASHRAE and IBPSA-USA Chicago, IL, Sep. 2018.
[36] L.M. Candanedo, V. Feldheim, D. Deramaix, A methodology based on Hidden Markov Models for occupancy detection and a case study in a low energy residential building, Energy Build. 148 (Aug. 2017) 327–341, https://doi.org/10.1016/j.enbuild.2017.05.031.
[37] N. Clements, R. Zhang, A. Jamrozik, C. Campanella, B. Bauer, The spatial and temporal variability of the indoor environmental quality during three simulated office studies at a living Lab, Buildings 9 (3) (Mar. 2019) 62, https://doi.org/10.3390/buildings9030062.
[38] S. Sadowski, P. Spachos, RSSI-based indoor localization with the Internet of Things, IEEE Access 6 (2018) 30149–30161, https://doi.org/10.1109/ACCESS.2018.2843325.
[39] C.G. Ryan, P.M. Dall, M.H. Granat, P.M. Grant, Sitting patterns at work: objective measurement of adherence to current recommendations, Ergonomics 54 (6) (Jun. 2011) 531–538, https://doi.org/10.1080/00140139.2011.570458.
[40] A.A. Thorp, et al., Prolonged sedentary time and physical activity in workplace and non-work contexts: a cross-sectional study of office, customer service and call centre employees, Int. J. Behav. Nutr. Phys. Activ. 9 (1) (2012) 128, https://doi.org/10.1186/1479-5868-9-128.
[41] R.E. Evans, H.O. Fawole, S.A. Sheriff, P.M. Dall, P.M. Grant, C.G. Ryan, Point-of-Choice prompts to reduce sitting time at work, Am. J. Prev. Med. 43 (3) (Sep. 2012) 293–297, https://doi.org/10.1016/j.amepre.2012.05.010.
[42] S.A. Clemes, R. Patel, C. Mahon, P.L. Griffiths, Sitting time and step counts in office workers, Occup. Med. 64 (3) (Apr. 2014) 188–192, https://doi.org/10.1093/occmed/kqt164.
[43] N. Owen, G.N. Healy, C.E. Matthews, D.W. Dunstan, Too much sitting: the population health science of sedentary behavior, Exerc. Sport Sci. Rev. 38 (3) (Jul. 2010) 105–113, https://doi.org/10.1097/JES.0b013e3181e373a2.
[44] C.L. Edwardson, et al., Effectiveness of the Stand More AT (SMArT) Work intervention: cluster randomised controlled trial, BMJ (Oct. 2018), k3870, https://doi.org/10.1136/bmj.k3870.
[45] D.M. Hallman, S.E. Mathiassen, H. Jahncke, Sitting patterns after relocation to activity-based offices: a controlled study of a natural intervention, Prev. Med. 111 (Jun. 2018) 384–390, https://doi.org/10.1016/j.ypmed.2017.11.031.
[46] B. Gardner, S. Dewitt, L. Smith, J.P. Buckley, S.J.H. Biddle, L. Mansfield, The ReSiT study (reducing sitting time): rationale and protocol for an exploratory pilot study of an intervention to reduce sitting time among office workers, Pilot Feasibility Stud. 3 (1) (Dec. 2017) 47, https://doi.org/10.1186/s40814-017-0191-2.
[47] S. Dewitt, et al., "Office workers' experiences of attempts to reduce sitting-time: an exploratory, mixed-methods uncontrolled intervention pilot study, BMC Publ. Health 19 (1) (Dec. 2019) 819, https://doi.org/10.1186/s12889-019-7196-0.
[48] E.N. Ussery, J.E. Fulton, D.A. Galuska, P.T. Katzmarzyk, S.A. Carlson, Joint prevalence of sitting time and leisure-time physical activity among US adults, J. Am. Med. Assoc. 320 (19) (Nov. 2018) 2036, https://doi.org/10.1001/jama.2018.17797, 2015-2016.
[49] B. Wallmann-Sperlich, J.Y. Chau, I. Froboese, Self-reported actual and desired proportion of sitting, standing, walking and physically demanding tasks of office employees in the workplace setting: do they fit together? BMC Res. Notes 10 (1) (Dec. 2017) 504, https://doi.org/10.1186/s13104-017-2829-9.
[50] Y. Al Horr, M. Arif, A. Kaushik, A. Mazroei, M. Katafygiotou, E. Elsarrag, Occupant productivity and office indoor environment quality: a review of the literature, Build. Environ. 105 (Aug. 2016) 369–389, https://doi.org/10.1016/j.buildenv.2016.06.001.
[51] T. Labeodan, K. Aduda, W. Zeiler, F. Hoving, Experimental evaluation of the performance of chair sensors in an office space for occupancy detection and occupancy-driven control, Energy Build. 111 (Jan. 2016) 195–206, https://doi.org/10.1016/j.enbuild.2015.11.054.
[52] J. Yang, M. Santamouris, S.E. Lee, Review of occupancy sensing systems and occupancy modeling methodologies for the application in institutional buildings, Energy Build. 121 (Jun. 2016) 344–349, https://doi.org/10.1016/j.enbuild.2015.12.019.
[53] T. Labeodan, W. Zeiler, G. Boxem, Y. Zhao, "Occupancy measurement in commercial office buildings for demand-driven control applications—a survey and detection system evaluation, Energy Build. 93 (Apr. 2015) 303–314, https://doi.org/10.1016/j.enbuild.2015.02.028.
[54] L.M. Candanedo, V. Feldheim, Accurate occupancy detection of an office room from light, temperature, humidity and CO_2 measurements using statistical learning models, Energy Build. 112 (Jan. 2016) 28–39, https://doi.org/10.1016/j.enbuild.2015.11.071.
[55] D. Calì, P. Matthes, K. Huchtemann, R. Streblow, D. Müller, CO_2 based occupancy detection algorithm: experimental analysis and validation for office and residential buildings, Build. Environ. 86 (Apr. 2015) 39–49, https://doi.org/10.1016/j.buildenv.2014.12.011.
[56] S. Kar, P.K. Varshney, Accurate estimation of indoor occupancy using gas sensors, in: In 2009 International Conference on Intelligent Sensor, Sensor Networks and Information Processing (ISSNIP), Melbourne, Australia, 2009, pp. 355–360, https://doi.org/10.1109/ISSNIP.2009.5416806.
[57] A. Ebadat, G. Bottegal, D. Varagnolo, B. Wahlberg, K.H. Johansson, Estimation of building occupancy levels through environmental signals deconvolution, in: Proceedings of the 5th ACM Workshop on Embedded Systems for Energy-Efficient Buildings - BuildSys'13, Italy, Roma, 2013, pp. 1–8, https://doi.org/10.1145/2528282.2528290.
[58] T.H. Pedersen, K.U. Nielsen, S. Petersen, Method for room occupancy detection based on trajectory of indoor climate sensor data, Build. Environ. 115 (Apr. 2017) 147–156, https://doi.org/10.1016/j.buildenv.2017.01.023.
[59] S.H. Ryu, H.J. Moon, Development of an occupancy prediction model using indoor environmental data based on machine learning techniques, Build. Environ. 107 (Oct. 2016) 1–9, https://doi.org/10.1016/j.buildenv.2016.06.039.
[60] M. Jin, N. Bekiaris-Liberis, K. Weekly, C. Spanos, A. Bayen, Sensing by proxy: occupancy detection based on indoor CO2 concentration, in: The 9th international conference on mobile ubiquitous computing, systems, services and technologies (UBICOMM 2015), July 2015, pp. 1–14.
[61] S. Wang, J. Burnet, H. Chong, Experimental validation of CO_2-based occupancy detection for demand-controlled ventilation, Indoor Built Environ. 8 (6) (Nov. 1999) 377–391, https://doi.org/10.1177/1420326X9900800605.
[62] A. Persily, L. de Jonge, Carbon dioxide generation rates for building occupants, Indoor Air 27 (5) (2017) 868–879, https://doi.org/10.1111/ina.12383.
[63] G. Pei, D. Rim, S. Schiavon, M. Vannucci, Effect of sensor position on the performance of CO2-based demand controlled ventilation, Energy Build. 202 (Nov. 2019), 109358, https://doi.org/10.1016/j.enbuild.2019.109358.
[64] M. Borgen Haugland, A. Yang, S.B. Holøs, K. Thunshelle, M. Mysen, Demand-controlled ventilation: do different user groups require different CO_2-setpoints? IOP Conf. Ser. Mater. Sci. Eng. 609 (Oct. 2019), 042062 https://doi.org/10.1088/1757-899X/609/4/042062.
[65] Pacific Northwest National Laboratory for the U.S. Department of Energy Building Energy Codes Program, 2012 IECC: Demand Control Ventilation, Energy Efficiency & Renewable Energy (Aug. 2012) (PNNL-SA-89859).
[66] X. Tang, P.K. Misztal, W.W. Nazaroff, A.H. Goldstein, Siloxanes are the most abundant volatile organic compound emitted from engineering students in a classroom, Environ. Sci. Technol. Lett. 2 (11) (Nov. 2015) 303–307, https://doi.org/10.1021/acs.estlett.5b00256.
[67] Y. Liu, et al., Characterizing sources and emissions of volatile organic compounds in a northern California residence using space- and time-resolved measurements, Indoor Air (May 2019), https://doi.org/10.1111/ina.12562 ina.12562.
[68] Y. Tian, et al., Fluorescent biological aerosol particles: concentrations, emissions, and exposures in a northern California residence, Indoor Air 28 (4) (Jul. 2018) 559–571, https://doi.org/10.1111/ina.12461.
[69] J. Kuutti, "A Test Setup for Comparison of People Flow Sensors," Licentiate Thesis, School of Electrical Engineering, Alto University, Mar 2012.
[70] C. Duarte, K. Van Den Wymelenberg, C. Rieger, Revealing occupancy patterns in an office building through the use of occupancy sensor data, Energy Build. 67 (Dec. 2013) 587–595, https://doi.org/10.1016/j.enbuild.2013.08.062.
[71] A.S. Ali, Z. Zanzinger, D. Debose, B. Stephens, Open Source Building Science Sensors (OSBSS): a low-cost Arduino-based platform for long-term indoor environmental data collection, Build. Environ. 100 (May 2016) 114–126, https://doi.org/10.1016/j.buildenv.2016.02.010.
[72] B.W. Hobson, D. Lowcay, H.B. Gunay, A. Ashouri, G.R. Newsham, Opportunistic occupancy-count estimation using sensor fusion: a case study, Build. Environ. 159 (Jul. 2019), 106154, https://doi.org/10.1016/j.buildenv.2019.05.032.
[73] W. Wang, J. Chen, G. Huang, Y. Lu, Energy efficient HVAC control for an IPS-enabled large space in commercial buildings through dynamic spatial occupancy distribution, Appl. Energy 207 (Dec. 2017) 305–323, https://doi.org/10.1016/j.apenergy.2017.06.060.
[74] V.L. Erickson, et al., Energy efficient building environment control strategies using real-time occupancy measurements, in: Proceedings of the First ACM Workshop on Embedded Sensing Systems for Energy-Efficiency in Buildings - BuildSys '09, Berkeley, California, 2009, p. 19, https://doi.org/10.1145/1810279.1810284.
[75] K.P. Lam, R. Shang, B. Andres, Y. Chiou, B. Dong, D. Benitez, Information-theoretic environmental features selection for occupancy detection in open offices, in: Eleventh International IBPSA Conference, July 2009, pp. 1460–1467. Glasgow, Scotland.
[76] Q. Huang, Z. Ge, C. Lu, "Occupancy estimation in smart buildings using audio-processing techniques,", in: International Conference on Computing in Civil and Building Engineering, Feb. 2016.
[77] W. Wang, J. Chen, T. Hong, Modeling occupancy distribution in large spaces with multi-feature classification algorithm, Build. Environ. 137 (Jun. 2018) 108–117, https://doi.org/10.1016/j.buildenv.2018.04.002.
[78] A. Braun, M. Majewski, R. Wichert, A. Kuijper, Investigating low-cost wireless occupancy sensors for beds, in: N. Streitz, P. Markopoulos (Eds.), ", Distributed, Ambient and Pervasive Interactions, vol. 9749, Springer International Publishing, Cham, 2016, pp. 26–34.
[79] R. Melfi, B. Rosenblum, B. Nordman, K. Christensen, "Measuring building occupancy using existing network infrastructure,", in: 2011 International Green Computing Conference and Workshops, Orlando, FL, USA, Jul. 2011, pp. 1–8, https://doi.org/10.1109/IGCC.2011.6008560.
[80] E. Naghiyev, M. Gillott, R. Wilson, Three unobtrusive domestic occupancy measurement technologies under qualitative review, Energy Build. 69 (Feb. 2014) 507–514, https://doi.org/10.1016/j.enbuild.2013.11.033.
[81] J. Wilson, N. Patwari, See-through walls: motion tracking using variance-based radio tomography networks, IEEE Trans. Mobile Comput. 10 (5) (May 2011) 612–621, https://doi.org/10.1109/TMC.2010.175.
[82] E. Sifuentes, R. González-Landaeta, J. Cota-Ruiz, F. Reverter, Microcontroller-based seat occupancy detection and classification, Proceedings 2 (13) (Nov. 2018) 1040, https://doi.org/10.3390/proceedings2131040.
[83] P. Blessy, R. Jegan, X.A. Mary, Seat occupancy detection based on impedance measurement, Int. J. Innovative Technol. Explor. Eng. 2 (4) (2013) 3.

[84] A.S. Zeeman, M.J. Booysen, G. Ruggeri, B. Lagana, Capacitive seat sensors for multiple occupancy detection using a low-cost setup,, in: IEEE International Conference on Industrial Technology (ICIT), Cape Town, Feb. 2013, 2013, pp. 1228–1233, https://doi.org/10.1109/ICIT.2013.6505849.

[85] K. Noro, R. Lueder, S. Yamada, G. Fujimaki, H. Oyama, Y. Hashidate, Revisiting Sitting Cross-Cultural Aspects of Seating,"Noro, Kageyu, et al. "Revisiting Sitting Cross-Cultural Aspects of Seating, in: ", Proceedings of the Human Factors and Ergonomics Society Annual Meeting, vol. 50, 2006, 7, Los Angeles, CA.

[86] L. Russell, R. Goubran, F. Kwamena, "Posture sensing using a low-cost temperature sensor array,", in: IEEE International Symposium on Medical Measurements and Applications (MeMeA), Rochester, MN, USA, May 2017, 2017, pp. 443–447, https://doi.org/10.1109/MeMeA.2017.7985917.

[87] R. Kumar, A. Bayliff, D. De, A. Evans, S.K. Das, M. Makos, "Care-Chair: sedentary activities and behavior assessment with smart sensing on chair backrest,", in: 2016 IEEE International Conference on Smart Computing, SMARTCOMP), St Louis, MO, USA, May 2016, pp. 1–8, https://doi.org/10.1109/SMARTCOMP.2016.7501682.

[88] L. Xu, G. Chen, J. Wang, R. Shen, and S. Zhao, "A sensing cushion using simple pressure distribution sensors," in 2012 IEEE International Conference on Multisensor Fusion and Integration for Intelligent Systems (MFI), Hamburg, Germany, Sep. 2012, pp. 451–456, doi: 10.1109/MFI.2012.6343048.

[89] H.Z. Tan, L.A. Slivovsky, A. Pentland, A sensing chair using pressure distribution sensors, IEEE ASME Trans. Mechatron. 6 (3) (Sep. 2001) 261–268, https://doi.org/10.1109/3516.951364.

[90] P. Orlewski, L. Federspiel, M. Cuddihy, M. Rao, S. Fuks, Advanced occupant detection system: detection of human vital signs by seat-embedded ferroelectric film sensors and by vibration analysis, in: 22nd Enhanced Safety of Vehicles Conference (NHTSA) (No.11-0205-W), 2011. http://wwwnrd.nhtsa.dot.gov/pdf/ESV/esv22/Session.203.

[91] J. Synnott, J. Rafferty, C.D. Nugent, Detection of workplace sedentary behavior using thermal sensors, in: 2016 38th Annual International Conference of the IEEE Engineering in Medicine and Biology Society (EMBC), Orlando, FL, USA, Aug. 2016, pp. 5413–5416, https://doi.org/10.1109/EMBC.2016.7591951.

[92] U.S. Department of Commerce, National Oceanic & Atmospheric Administration, National environmental satellite, data, and information service. Object name record of climatological observations, 09/10/2020. [Online]. Available at, https://www.ncdc.noaa.gov/cdo-web/datasets/.

[93] R. Yu, M. Burke, N. Raad, Exploring impact of future flexible working model evolution on urban environment, economy and planning, J. Urban Manag. 8 (3) (Dec. 2019) 447–457, https://doi.org/10.1016/j.jum.2019.05.002.